Effects of Y27632 on Aqueous Humor Outflow Facility With Changes in Hydrodynamic Pattern and Morphology in Human Eyes

Chen-Yuan Charlie Yang,[1,2] Ye Liu,[3] Zhaozeng Lu,[4] Ruiyi Ren,[1,2] and Haiyan Gong[1,2]

[1]Department of Anatomy and Neurobiology, Boston University School of Medicine, Boston, Massachusetts
[2]Department of Ophthalmology, Boston University School of Medicine, Boston, Massachusetts
[3]Department of Pathology, The First Hospital of Jilin University, Changchun, China
[4]Department of Ophthalmology, Huashan Hospital of Fudan University, Shanghai, China

Correspondence: Haiyan Gong, Department of Ophthalmology, Boston University School of Medicine, 72 East Concord Street, Room L-905, Boston, MA 02118; hgong@bu.edu.

C-YCY and YL contributed equally to the work presented here and should therefore be regarded as equivalent authors.

Submitted: September 7, 2012
Accepted: July 30, 2013

Citation: Yang C-YC, Liu Y, Lu Z, Ren R, Gong H. Effects of Y27632 on aqueous humor outflows facility with changes in hydrodynamic pattern and morphology in human eyes. *Invest Ophthalmol Vis Sci.* 2013;54:5859–5870. DOI:10.1167/iovs.12-10930

Purpose. To determine the effect of Y27632, a Rho-kinase inhibitor on aqueous outflow facility, flow pattern, and juxtacanalicular tissue (JCT)/trabecular meshwork (TM) morphology in human eyes.

Methods. Sixteen enucleated human eyes were perfused with PBS plus glucose (GPBS) at 15 mm Hg to establish the baseline outflow facility. Six eyes were perfused for short-duration (30 minute) with either 50 μM Y27632 or GPBS ($n = 3$ per group). Ten eyes were perfused for long duration (3 hours) with either 50 μM Y27632 or GPBS ($n = 5$ per group). Outflow pattern was labeled using fluorescent microspheres, and effective filtration length (EFL) was measured. Morphologic changes and their relationship to EFL and facility were analyzed.

Results. Outflow facility significantly increased after short-duration perfusion with Y27632 compared with its own baseline ($P = 0.03$), but did not reach statistical significance compared with its controls ($P = 0.07$). Outflow facility ($P = 0.01$) and EFL ($P < 0.05$) were significantly increased after long-duration perfusion with Y27632 compared with its controls. Increases in outflow facility and EFL demonstrated a positive correlation. Morphologically, the TM and JCT of high-tracer regions were more expanded compared with low-tracer regions. A significant increase in JCT thickness was found in the long-duration Y27632 group compared with its control group (10.0 vs. 8.0 μm, $P < 0.01$).

Conclusions. Y27632 increases outflow facility in human eyes. This increase correlates positively with an increase in EFL, which is associated with an increased expansion in the JCT. Our data suggest that EFL could serve as a novel parameter to correlate with outflow facility.

Keywords: trabecular meshwork, rho-kinase inhibitor, Y27632, outflow facility, effective filtration area, morphology, light, confocal and electron microscopy

Primary open angle glaucoma is a leading cause of blindness worldwide. The primary risk factor associated with POAG is elevated IOP, consequent of high levels of aqueous humor outflow resistance.[1,2] Although the exact mechanism behind increased outflow resistance in POAG remains unclear,[2,3] the consensus is that the principal resistive sites lie in the trabecular meshwork (TM) outflow pathway proximal to upstream of Schlemm's canal (SC), consisting of the inner wall endothelium and its underlying TM.[4,5] However, the mechanism regulating outflow resistance remains elusive. Currently, reduction of IOP by medical or surgical means remains the sole approach for treatment of this disease. However, none of the first-line medical options available for patients target the TM outflow pathway, believed to be the site where the initial problem arises.

Over the last decade, several agents have been used to target the cytoskeleton of the cells in the TM outflow pathway, including cytochalasin,[6–8] latrunculin-B,[9,10] H-7,[11,12] and Y27632,[13–17] which augment aqueous humor outflow. Together, these agents have shown aqueous humor outflow resistance and IOP can be modulated through actomyosin cytoskeleton reorganization. Y27632 has been identified as a selective inhibitor for the Rho-associated coiled coil-forming kinase (ROCK), which regulates myosin light chain (MLC) phosphorylation by increasing MLC-phosphatase activity and decreasing MLC phosphorylation.[18–20] As a result, cells become less contractile and decrease the quantity of actin stress fibers and focal adhesions.[13,15] Studies have shown that Y27632 increases outflow facility in nonhuman models, including live rabbits[13,17] and monkeys,[16] and enucleated porcine,[15] bovine,[14] and monkey eyes.[21] Common morphologic features observed alongside increased outflow facility include the expansion of the subendothelial extracellular matrix within juxtacanalicular tissue (JCT), inner wall endothelium and JCT separation, and distension of inner wall endothelium. Similar structural changes were observed when using other cytoskeletal disrupting agents in nonhuman eyes as well.[8,10]

Similar hydrodynamic and morphologic changes were reported in the aqueous humor outflow pathway after washout induced and Y27632 treatment in both bovine and monkey eyes.[14,21,22] Studies have shown that human eyes do not exhibit washout effect[23,24]; in addition, other studies in enucleated

human eyes have demonstrated that more than 2 hours of perfusion with either H-7[11] or latrunculin-B[9] resulted in a much smaller increase in outflow facility (37% and 64%, respectively) compared with the 2- to 4-fold increase in outflow facility observed in nonhuman eyes.[8,10,12,25] Therefore, it is important to understand whether similar differences in outflow facility also exist between human and nonhuman eyes after Y27632 treatment.

The goals of this study are to determine the effects of Y27632 on aqueous humor outflow facility, hydrodynamic pattern, and morphology in enucleated human eyes. We hypothesize that similar to that in nonhuman eyes, an increase in outflow facility after Y27632 treatment is positively correlated with an increase in effective filtration length (EFL) in human eyes, which is regulated by morphologic changes; however, it may take more time for human eyes to respond after Y27632 treatment. To test our hypothesis, we perfused Y27632 for a short duration (30 minutes) under similar experimental conditions as our previous studies in bovine and monkey eyes.[14,21] In addition, we perfused the eyes with Y27632 for a longer duration (3 hours). Fluorescent microspheres and confocal microscopy were used to visualize the change in outflow pattern, and light and electron microscopy were employed to investigate the morphologic changes.

Materials and Methods

Materials

Sixteen enucleated human eyes from anonymous donors without any known history of ocular diseases were obtained from National Disease Research Interchange (Philadelphia, PA) and Lions Eye Institute for Transplant & Research, Inc. (Tampa, FL). The mean donor age was 70 years (range, 43–90), and the mean postmortem time to the start of perfusion was 22 hours (all except 2 eyes were within 24 hours, range, 16–34). Each eye was confirmed to be grossly healthy by examination under a dissecting microscope.

The perfusate was Dulbecco's phosphate-buffered saline (pH 7.3; Invitrogen, Grand Island, NY) containing 5.5 mM D-glucose (collectively referred to as GPBS). Red carboxylate-coated fluorescent microspheres (500 or 200 nm, Invitrogen) at 0.002% vol/vol concentration were used to trace aqueous humor outflow patterns. The specific sizes and concentration of fluorescent microspheres were chosen for negligible obstruction of aqueous outflow through the TM.[26] To maintain consistency with our previous studies in bovine[14] and monkey,[21] a 50-μM concentration of Y27632 (Calbiochem, La Jolla, CA) in GPBS concentration was used in this study.

Methods

Ocular Perfusion

The perfusion procedure was described in detail in our previous work.[22] All eyes were initially perfused with GPBS for 30 minutes at 15 mm Hg to establish a stable baseline facility. Anterior chamber fluid from each eye was exchanged with either 5 mL of 50 μM Y7632 or GPBS, followed by perfusion of the same solution for 30 minutes (short duration, $n = 3$ per group) or 3 hours (long duration, $n = 5$ per group). To label the hydrodynamic outflow, anterior chamber fluid from all eyes was then exchanged for 5 mL of GPBS containing fluorescent microspheres followed by fixed volume perfusion of the same solution. Anterior chamber fluid from all eyes was then exchanged and perfusion fixed at 15 mm Hg with a modified Karnovsky's fixative (2.5% glutaraldehyde and 2% paraformaldehyde, pH 7.3). After perfusion was completed, eyes were hemisected along the equator and immersed overnight in the same fixative for further processing.

Confocal Microscopy

All fixed eyes were cut through the equator, and the vitreous body and lens of each eye were carefully removed. Anterior segments of the eyes were then divided into four quadrants (temporal, nasal, superior, and inferior). Each quadrant was cut into frontal sections, along a plane tangential to the corneoscleral limbus and perpendicular to the ocular surface.[14,27] To visualize cell nuclei, sections were counter stained with TO-PRO-3 or DAPI (Invitrogen, Carlsbad, CA). After three washes with PBS, sections were mounted and examined using a confocal microscope (Carl Zeiss 510, Axiovert 100M Laser Scanning Microscope; Carl Zeiss, Heidelberg, Germany) for image scanning and capturing. Fluorescent microspheres were visualized using a multi-track channel system with a 20× objective lens. Images were taken in all sections containing SC, so that the distribution of the tracer along the inner wall and the TM could be properly analyzed.

Effective filtration length is the one-dimensional equivalent to effective filtration area; this was measured as previously described.[14,21,22] The total length (TL) of the inner wall and fluorescent-decorated length (FL) of the inner wall in each image were measured using LSM Image Browser (Version 4.2; Carl Zeiss), and the average percent effective filtration length ($\sum$EFL/$\sum$TL) in each eye was calculated (Fig. 1A). A minimum of 16 images per eye from all four quadrants were measured and analyzed.

Trabecular meshwork thickness (the length from the innermost uveoscleral beam to the inner wall endothelium of SC) was measured to determine the effect of Y27632 on "relaxing" the TM. Confocal images of long-perfusion Y27632 and long-perfusion GPBS from previous EFL measurements were randomly selected (including both anterior and posterior parts of TM) and only included for measurement if the whole meshwork was observed. TM was designated as either a high-tracer (EFL $\geq$ 60%) or low-tracer (EFL $\leq$ 40%) region. Each image was measured at three different locations, and the average thickness of TM in high-tracer and low-tracer regions of each eye was then calculated and analyzed (Fig. 1B). Tissue sections analyzed by confocal microscopy were further processed for light and electron microscopy.

Light Microscopy

Tissue sections were post fixed in 2% osmium tetroxide and 1.5% potassium ferrocyanide for 2 hours, dehydrated in an ascending series of ethanol, and embedded in Epon-Araldite. Semithin sections (3 μm) were cut and stained with 1% Toluidine Blue (Fisher Scientific, Pittsburgh, PA). Light micrographs were taken using a 20× objective along the inner wall of SC. All the measurements described below were taken from eight tissue sections per eye from a minimum of three quadrants (accounting for a SC length between 7.6–12.5 mm per eye) of all eyes with long-duration perfusion with either Y27632 or GPBS. Juxtacanalicular tissue was defined as the tissue underlying SC, extending from SC endothelial cells to the empty space adjacent to the first trabecular beams.[28,29] The average JCT thickness ($\sum$JCT area/$\sum$JCT length), percent JCT empty space ($\sum$empty space/$\sum$JCT area,

Investigative Ophthalmology & Visual Science

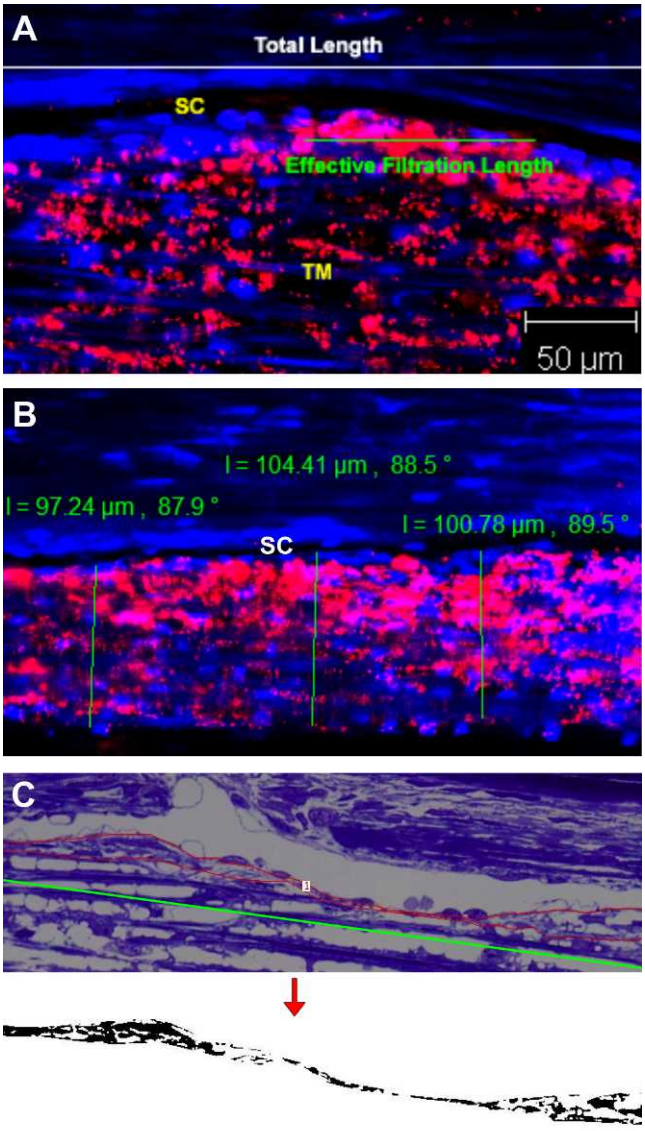

FIGURE 1. Measurement methods. (**A**) Measurement of the percent effective filtration length. The *green line* represents effective filtration length, and the *white line* represents TL of the inner wall of SC. The *red* represents the tracer distribution. The average percent effective filtration length (∑EFL/∑TL) in each eye was calculated. (**B**) Measurement of TM thickness. The *green line* represents the width of TM from innermost uveoscleral beam to the inner wall endothelium of SC. The *red* represents the tracer distribution. (**C**) Morphologic analysis of JCT. The *red line* represents the JCT area, and the *green line* represents the length of JCT. Juxtacanalicular tissue area was converted to binary image (*below*) to obtain the percent JCT empty space. The average JCT thickness (∑JCT area/∑JCT length) and percent JCT optically empty space (∑JCT optically empty space/∑JCT area) of each eye were calculated.

determined using a custom written ImageJ [National Institutes of Health, Bethesda, MD] macro) and loose JCT thickness (average JCT thickness × percent JCT empty space) of each eye were calculated (Fig. 1C). Giant vacuoles (GV) were identified if their diameter was greater than or equal to 2 µm and appearance was "smooth-walled, round, oval, reniform, or crescentic spaces."[30] Giant vacuoles were counted along the inner wall of SC and the number of GV per millimeter of SC length (∑GV number/∑SC length) was calculated. All the images were taken and measured in a masked manner to avoid biased analysis.

Electron Microscopy

Ultrathin sections (90 nm) were cut with an ultramicrotome (Ultracut E; Reichert-Jung, Leica, Wetzlar, Germany) counterstained with uranyl acetate and lead citrate, and examined using transmission electron microscopes (Philips EM300, Eindhoven, Netherlands; or JEOL JEM-1011, Tokyo, Japan). Electron micrographs were taken randomly at different quadrants along the inner wall of the SC. Morphology of the inner wall and JCT were analyzed and compared. The average JCT thickness of high-tracer and low-tracer regions was calculated from pooled images ($n = 107$) from all eyes (∑JCT area/∑JCT length) and compared between the Y27632 and GPBS groups. In region where fluorescent tracers were observed on both basal and apical side of the SC endothelium, serial sections were performed to understand how tracer crosses the pores of the SC inner wall, where pores are considered paracellular pores if cell–cell junctions were observed, otherwise they are considered intracellular pores.

Statistical Methods

Two-tailed Student's *t*-test and linear regression analysis were applied with a required significance level of P less than or equal to 0.05. All data are expressed as means ± SEM.

RESULTS

Outflow Facility

The outflow facility for the short-duration (30 minutes) Y27632 and GPBS groups ($n = 8$ each) were calculated by combining the 30 minute data points from both short-duration ($n = 3$ each) and long-duration groups ($n = 5$ each). An increase in outflow facility in the short-duration Y27632 group (29.0 ± 10.6%) was higher than in the GPBS group (5.2 ± 4.5%), but not reached statically significance ($P = 0.07$, unpaired *t*-test) (Fig. 2A). However, outflow facility was found significantly increased in the short-duration Y27632 group compared with its own baseline facility ($P = 0.03$, paired *t*-test) (Fig. 2B).

A significant increase in outflow facility was found following the long-duration (3 hours) of Y27632 treatment (60.6 ± 16.9%) compared with the GPBS group (–8.0 ± 9.1%) ($P = 0.01$, unpaired *t*-test, Fig. 2A) and compared with its own baseline ($P < 0.05$, paired *t*-test) (Fig. 2B). In contrast, perfusion with GPBS for 3 hours had no significant differences in outflow facility compared with its own baseline ($P = 0.5$, paired *t*-test, Fig. 2B).

Flow Pattern and Trabecular Meshwork Thickness

Segmental distributions of tracers in TM were observed in all eyes (Figs. 3A, 3C, 3E, 3G versus 3B, 3D, 3F, 3H). Fluorescent tracers often reached the inner wall of SC at the region near the collector channels, rather than the regions farther away from them. However, not all the inner wall regions adjacent to the collector channels had tracers pass through (Figs. 3B, 3F). The long-duration Y27632 group displayed an overall increase in tracer quantity and area along the inner wall of SC compared with the control group (Fig. 3). Confocal image analysis revealed that long-duration Y27632 has significantly higher EFL compared with long-duration GPBS and short-duration Y27632 groups (63.6 ±

Investigative Ophthalmology & Visual Science

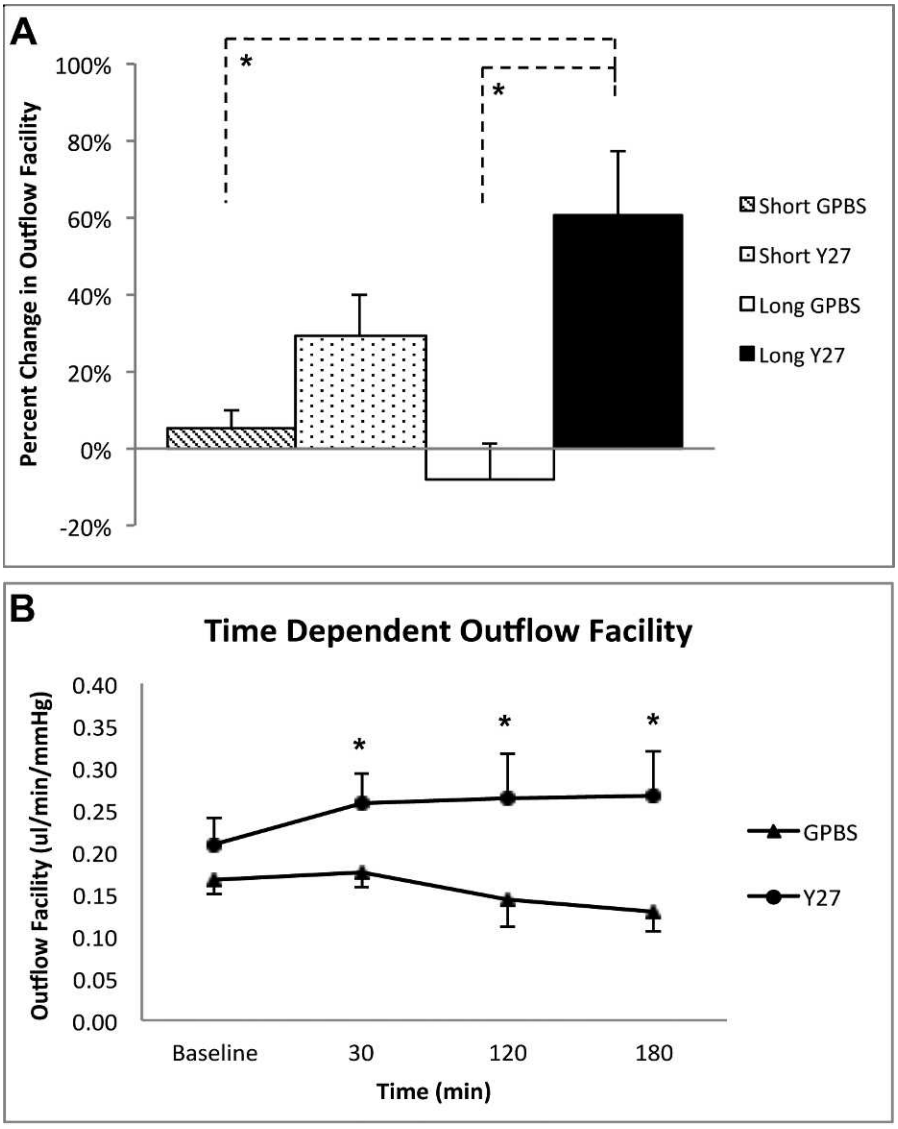

Figure 2. Outflow facility. (**A**) Changes in outflow facility between Y27632-treated groups (both 3 hours and 30 minutes) and their respective GPBS controls. An increase in outflow facility was observed in short-duration Y27632 group compared with the GPBS group ($n = 8$ for each group, 29.0 ± 10.6% vs. 5.2 ± 4.5%), but this increase did not reach statistical significance ($P = 0.07$, unpaired *t*-test). A significant increase in outflow facility was found after 3 hours perfusion with Y27632 compared with long- and short-duration control groups ($P < 0.05$, unpaired *t*-test). (**B**) Time-dependent changes of outflow facility between long-duration Y27632-treated and control eyes. The Y27632 group had a significant increase in outflow facility at 30 minutes ($n = 8$), 120 minutes ($n = 5$), and 180 minutes ($n = 5$) of perfusion with respect to their baseline ($P < 0.05$, paired *t*-test). In contrast, perfusion with GPBS at all time points had no significant differences in outflow facility compared to its own baseline ($P > 0.05$, paired *t*-test, Fig. 2B). Data are means ± SEM. *$P < 0.05$.

5.8 vs. 46.2 ± 4.8 vs. 39.9 ± 5.8%) (Fig. 4A). No significant difference in EFL was found between short-duration Y27632 and its control groups. On average, long-duration Y27632 increased EFL by 38% compared with its control. Moreover, TM thickness was found to increase in the high-tracer region compared with low-tracer region in both long-duration GPBS (95.7 ± 6.5 vs. 82.1 ± 5.8 μm, $P = 0.023$) and long-duration Y27632 (92.0 ± 6.3 vs. 73.7 ± 4.8 μm, $P < 0.01$) (Figs. 3, 4B).

Morphology of the Inner Wall of SC and Juxtacanalicular Tissue

To determine the Y27632 associated inner wall/JCT structural changes, we analyzed on average 26% (range, 21%–30%) of SC circumference and its underlying JCT per eye (based on 36 mm in SC circumference[31]) using bright field microscopy. While no obvious inner wall/JCT separation was observed at light microscopy level, JCT expansion can be seen in a few regions along the SC in both long-duration Y27632 and long-duration GPBS groups (Fig. 5A). Detailed morphologic analysis showed that average JCT thickness was significantly higher in the long-duration Y27632 group compared with the long-duration GPBS group (10.0 ± 0.5 vs. 8.0 ± 0.3 μm, $P < 0.01$, Fig. 5B). However, there were no significant differences in JCT optically empty space (GPBS: 40.0 ± 3.7 vs. Y2732: 44.83 ± 4.3%, $P > 0.05$) or GV numbers (GPBS: 17 ± 3 vs. Y27632: 19 ± 3 per mm SC length, $P > 0.05$) between these two groups.

By electron microscopy, we were able to visualize fluorescent tracers at the JCT regions and found that tracers accumulate mostly at loose JCT regions (more optically

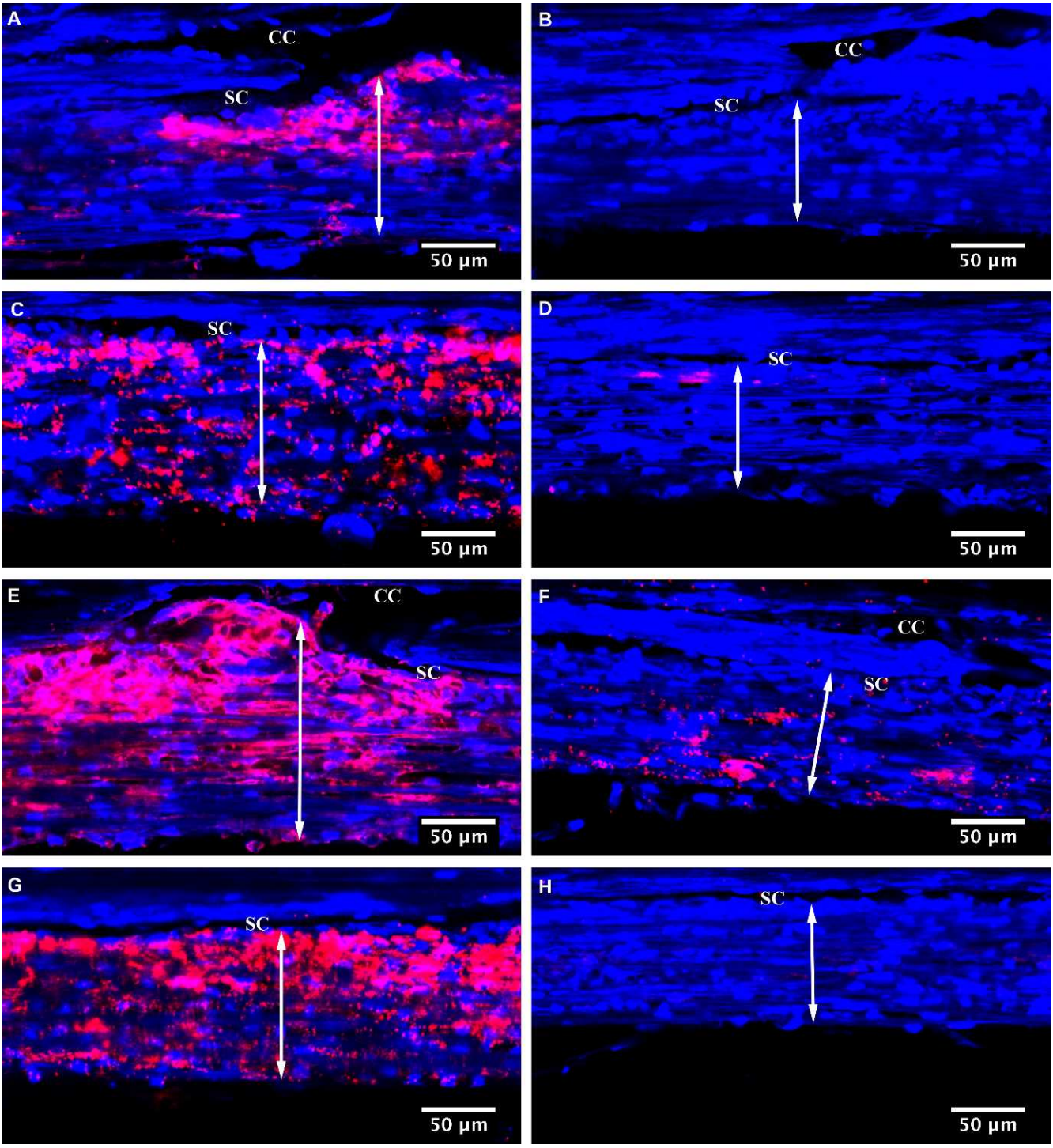

Figure 3. Tracer-decorated aqueous outflow pattern. Aqueous outflow pattern through the TM region with or without collector channel (CC) in Y27632-treated and control eyes. Segmental distribution of fluorescent tracer was observed along the SC in both control (**A**–**D**) and Y27632-treated eyes (**E**–**H**). An increased TM thickness (*double arrow*) was found in the high-tracer (**A**, **C**, **E**, **G**) compared with the low-tracer regions (**B**, **D**, **F**, **H**). More fluorescent tracers were found near some CC ostia (**A**, **E**), but not the other regions near CC ostia (**B**, **F**).

empty space), while fewer tracers and pigments accumulate at the dense JCT regions (Fig. 6A). This indicated that high-tracer regions (more flow) were predominately loose JCT regions. Further analysis showed that an increased JCT thickness in the high-tracer regions compared with low-tracer regions for both long-duration Y27632 (high-tracer: 8.6 ± 0.8 μm, $n = 24$ vs. low-tracer: 6.1 ± 0.6 μm, $n = 33$; $P < 0.05$) and GPBS (high-tracer: 10.2 ± 0.9 μm, $n = 15$ vs. lower-tracer 3.9 ± 0.3 μm, $n = 35$; $P < 0.001$) groups (Fig. 6B). Furthermore, the low-tracer regions of the Y27-treated eyes have significantly higher JCT thickness compared with the GPBS group ($P < 0.01$) (Fig. 6B). In some JCT expansion regions, separation between the inner wall and JCT was observed. Interestingly, when we carefully examined the

Investigative Ophthalmology & Visual Science

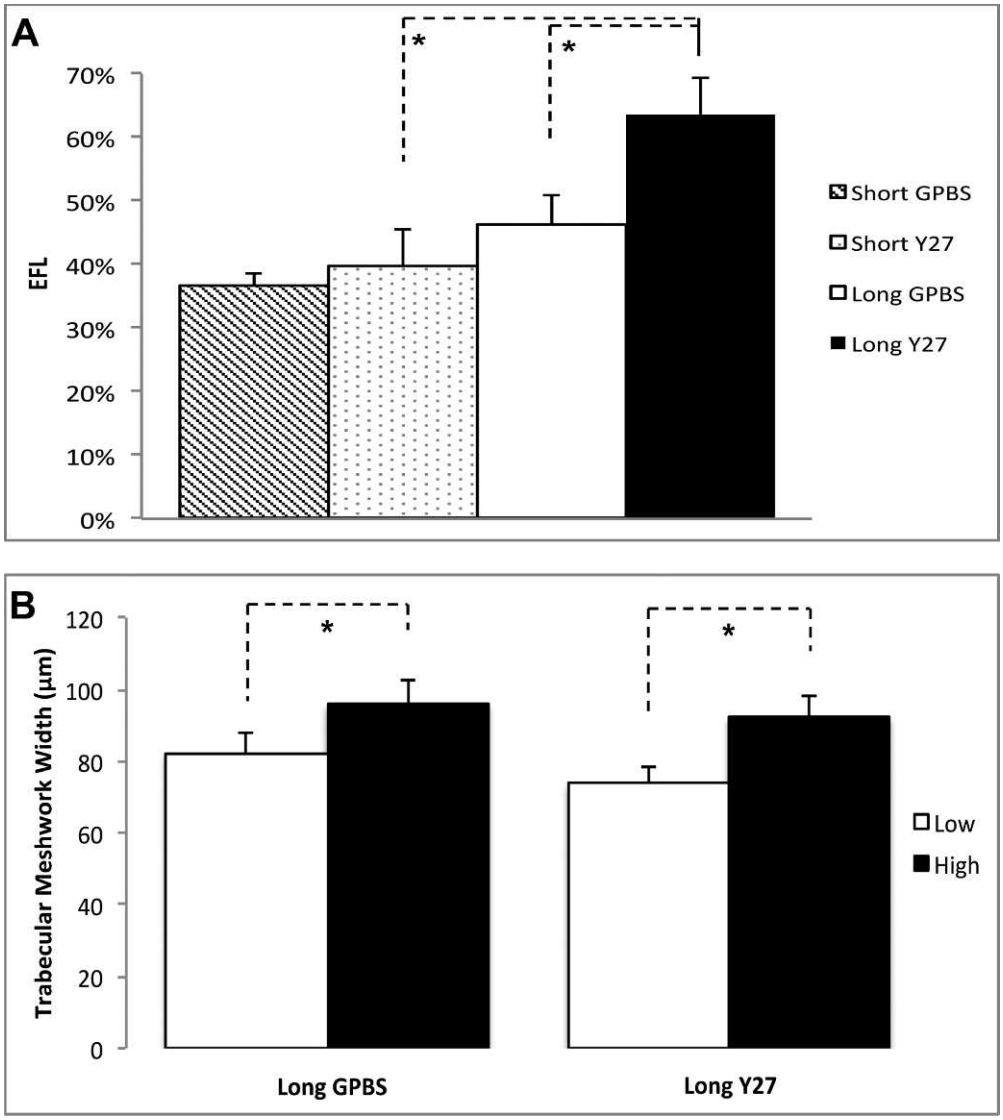

FIGURE 4. Confocal microscopic analysis. (**A**) Average percent EFL in Y27632-treated and control eyes. A significant increase in EFL was found in long-duration Y27632-treated eyes compared with the controls ($P < 0.05$). (**B**) Trabecular meshwork thickness (the length from the innermost uveoscleral beam to the inner wall endothelium). A significant increase of TM thickness in both long-duration Y27632 and long-duration control groups was found in the high-tracer regions than the low-tracer regions ($P < 0.05$).

serial sections of the areas ($n = 15$) where tracers located on both basal and apical side of the SC endothelium, we found pores in all of these areas; and they were all identified as paracellular pores (Figs. 7A–C).

Regression Analysis

Linear regression analysis showed that a significant positive correlation was found between EFL and change in outflow facility (with respect to baseline outflow facility) ($R^2 = 0.511$, $P = 0.002$) (Fig. 8A). Furthermore, a strong positive correlation was found between loose JCT thickness and change in outflow facility ($R^2 = 0.435$, $P = 0.038$) (Fig. 8B).

DISCUSSION

In this study, we investigated the effects of Y27632, a Rho-kinase inhibitor, on aqueous humor outflow facility, flow pattern (EFL), and morphology after 30 minutes and 3 hours perfusion in human eyes to test our hypothesis that EFL is positively correlated with outflow facility, which is regulated by morphologic changes. Our major findings are that (1) a significant increase in outflow facility was found after 30 minutes of perfusion with Y27632 compared with its own baseline in enucleated human eyes; however, it took a longer time (3 hours) for this increase in outflow facility to reach statistical significance compared to its control group, (2) the increase in outflow facility correlates positively with an increase in EFL, which is associated with an increased JCT thickness compared with the controls, and (3) aqueous humor outflow through the TM is segmental in human eyes, and an increased TM and JCT thickness was found in high-tracer regions compared with low-tracer regions. Our data confirmed our hypothesis that an increase in outflow facility by Y27632 is positively correlated with an increase in EFL, which is regulated by morphologic changes.

Previous studies have shown that Y27632 significantly increases outflow facility in nonhuman eyes after 30 minutes perfusion compared with their controls.[14,21] This study

Investigative Ophthalmology & Visual Science

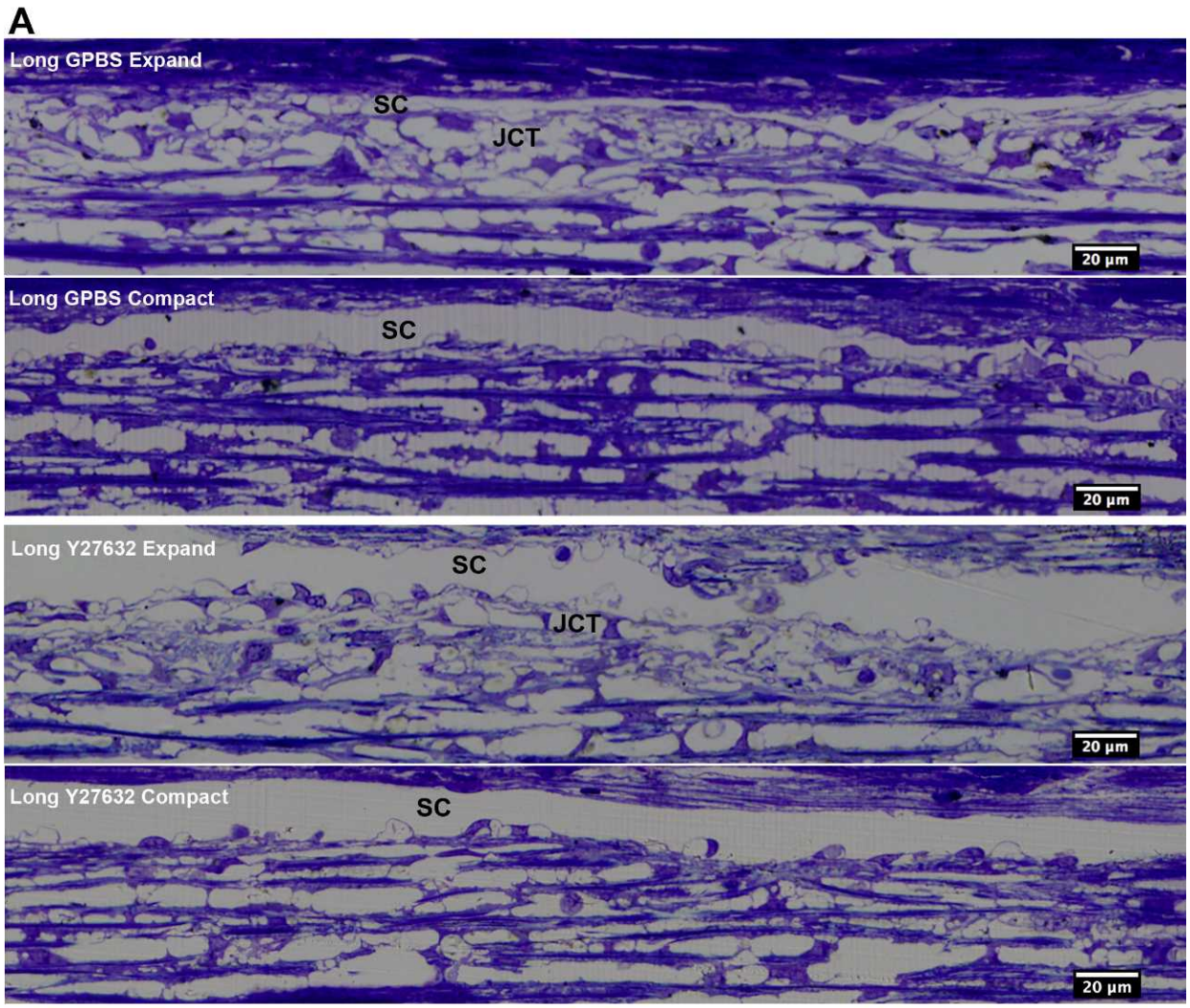

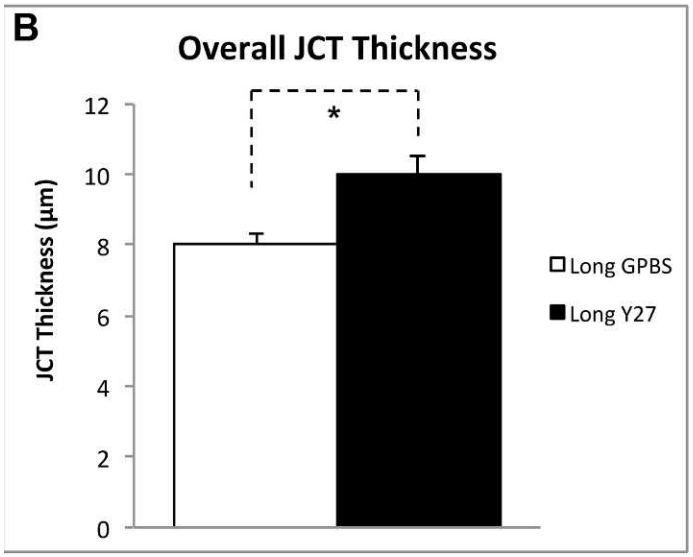

FIGURE 5. Light microscopic analysis. (**A**) Morphological comparison. Juxtacanalicular tissue expansion and compact regions were observed in both long-duration GPBS and long-duration Y27632 groups. (**B**) Juxtacanalicular tissue thickness. A significant increase in average JCT thickness was found in long-duration Y27632 group compared with its control ($P < 0.01$).

Investigative Ophthalmology & Visual Science

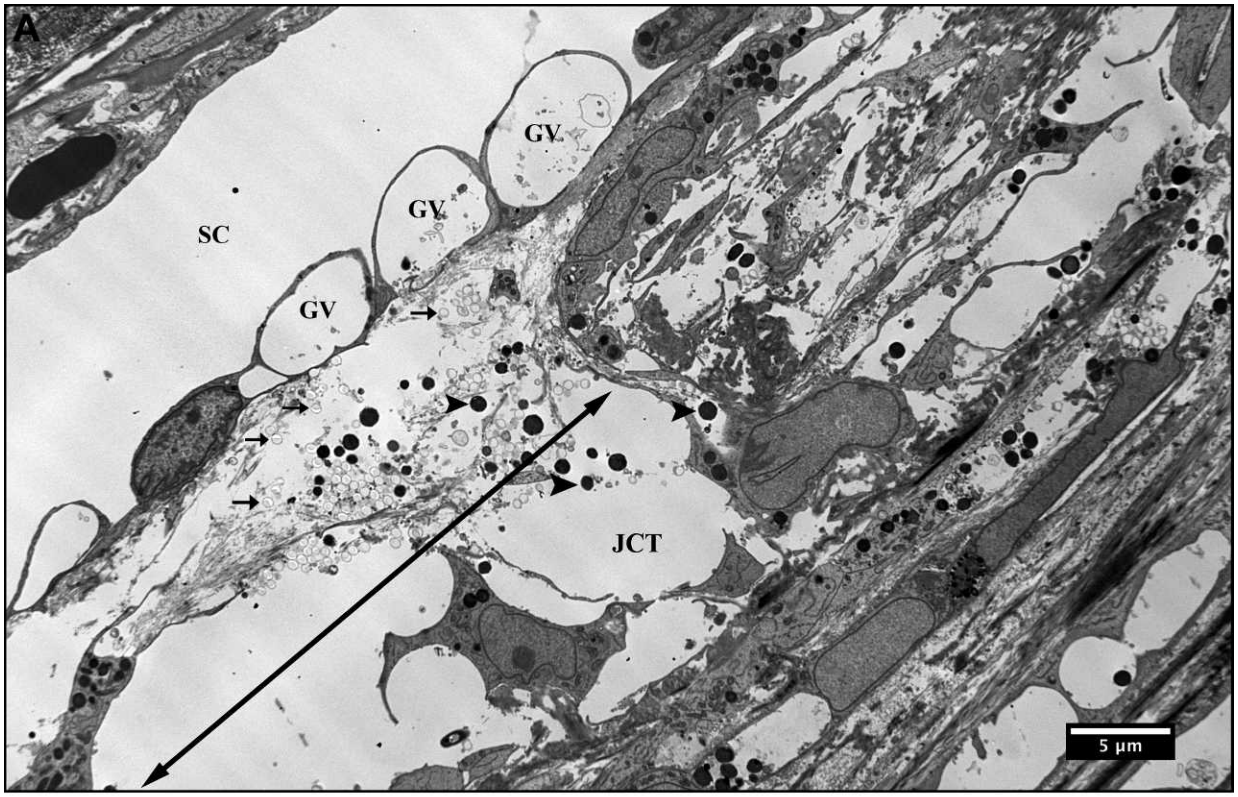

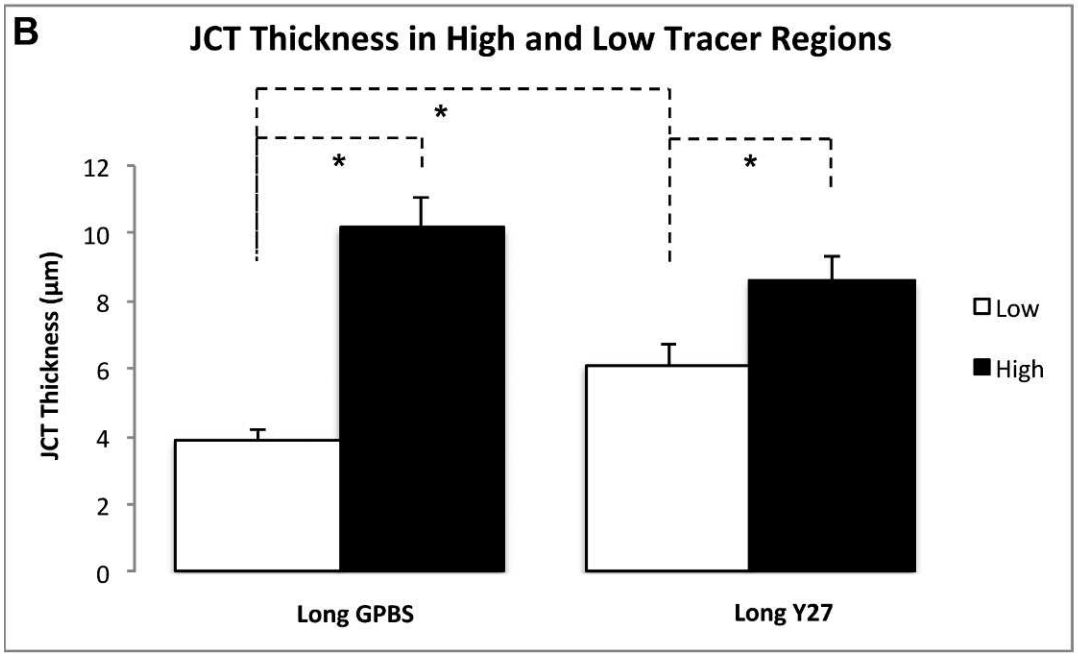

Figure 6. Electron microscopic analysis. (**A**) Fluorescent microspheres (*arrows*) and pigments (*arrowheads*) were seen in the loose JCT region, which contains larger optical empty space (*double arrow*) than dense JCT (*nondouble arrow*). No fluorescent microspheres were seen in the GV. (**B**) Juxtacanalicular tissue thickness in high- and low-tracer regions. High-tracer regions had significantly higher JCT thickness compared with low-tracer regions in both long-duration Y27632 and GPBS groups ($P < 0.05$). Y27632 group had significantly higher JCT thickness compared with GPBS group at low-tracer regions ($P < 0.01$), while no difference was found at high-tracer regions.

demonstrated that although a significant increase in outflow facility was observed after 30 minutes perfusion with Y27632 in human eyes compared with its baseline, a longer perfusion time (3 hours) was necessary for Y27632 to significantly increase outflow facility to the level comparable with nonhuman eyes[14,21] compared with its controls (Fig. 9A). This increase in outflow facility is associated with an increase in EFL. Effective filtration length was shown previously by our group to be an important parameter correlated with aqueous outflow facility in nonhuman species.[14,21,22,32,33] Analysis of

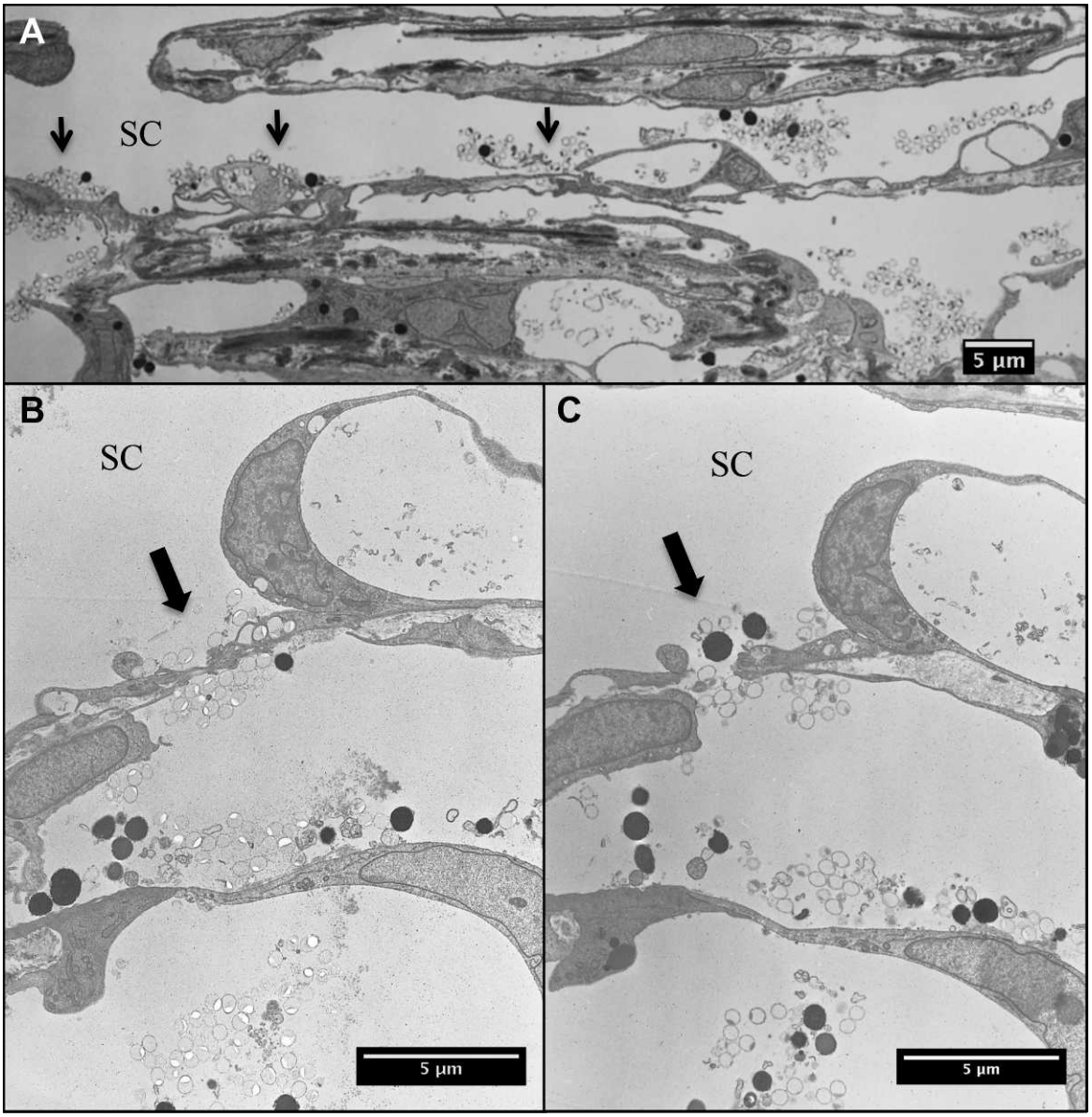

FIGURE 7. Analysis of tracer crossing the inner wall. (**A**) Tracers were observed across the inner wall of SC at various regions (*arrows*) at lower magnification. (**B**) At a higher magnification, fluorescent tracers were observed on both basal and apical side of a cell–cell junction in the inner wall endothelium of SC. (**C**) Serial sections were cut in the same cell–cell junction region shown as (**B**). (**A**) Paracellular pore was seen with tracers on both basal and apical side.

the EFL demonstrated a significant increase in long Y27632-treated eyes compared with long-GPBS or short-Y27632 groups (Fig. 4A), suggesting a more uniform distribution of flow can lead to a greater overall outflow facility. We also noted that the EFL increase (with respective controls) in human eyes is also smaller compared with bovine[14] and monkey[21] eyes (Fig. 9B), which explains the smaller increase of outflow facility in human eyes compared with nonhuman eyes. Furthermore, our results demonstrated a positive correlation between EFL and an increase in outflow facility ($R^2 = 0.511$) in human eyes, which is similar to our previous studies with Y27632 in bovine ($R^2 = 0.381$)[14] and monkey ($R^2 = 0.375$)[21] eyes. We have previously documented that a decrease in outflow facility in acute and chronic elevation of IOP in bovine[32] and monkey[34] eyes was correlated with a decrease in EFL. Additionally, an inverse correlation between EFL and IOP was recently reported in an ocular hypotensive mouse model.[33] Collectively, our current and previous results suggest that the EFL is a valuable parameter to correlate with outflow facility and IOP across species.

Studies in nonhuman eyes have shown that drug-induced increases in outflow facility[10,12,14,15,21] share several common morphologic features, including inner wall/JCT separation, JCT expansion, and increased in GV number. Interestingly, unlike our previous studies in nonhuman eyes, where distinct inner wall/JCT separation can be observed by viewing the images at the light microscopy level, we were unable to distinguish morphologic changes using the same method as we did previously. Instead, morphologic analysis on the average JCT thickness was employed, which was determined by dividing the measured total JCT area by the total JCT length per eye. This result showed that 3 hours of Y27632 treatment in human eyes induced expansion of the JCT by an average of 2 μm compared with its controls. Further analysis of JCT with

Investigative Ophthalmology & Visual Science

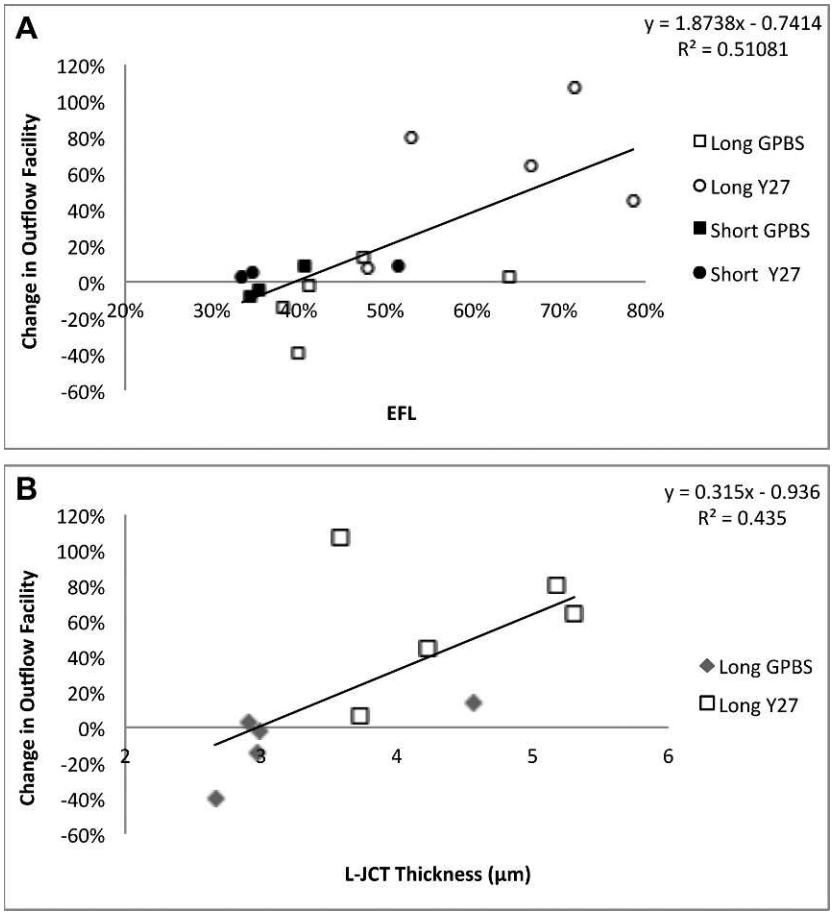

Figure 8. Linear regression analysis. (**A**) A significant positive correlation was found between percent EFL and change in outflow facility (with respect to baseline). (**B**) A significant positive correlation was found between loose JCT (L-JCT) thickness and change in outflow facility (with respect to baseline).

electron microscopy revealed that high-tracer (more flow) regions have significantly higher average JCT thickness compared with low-tracer regions in both Y27632 and control groups. In addition, while there were no differences in JCT thickness of the high-tracer regions between Y27632 and control groups, the Y27632 group had higher JCT thickness at the low-tracer regions compared with its controls. Together, the data suggests that overall JCT thickness increased following Y27632 treatment was the combination of an increase in high-tracer regions as well as increased JCT thickness at the low-tracer regions. Our data also demonstrated that loose JCT thickness was strongly correlative with changes in outflow facility ($R^2 = 0.435$, $P = 0.038$). Therefore, our results showed that the morphologic change of increased expansion in the JCT is associated with increases in outflow facility and EFL, which is a similar change found in bovine and monkey eyes but to a lesser degree, which explained a less significant increase in outflow facility after Y27632 treatment in human eyes compared with nonhuman eyes. Additionally, our morphologic findings support the funneling hypothesis,[4] that the bulk of outflow resistance is generated within the JCT and that the attachment between the inner wall and JCT plays an important role in regulating outflow resistance. In this study, the overall GV numbers were similar between long-term Y27632 treatment and its control groups, which differs from previous studies in nonhuman eyes,[14,15,21,35] where GV number were increased in Y27632-treated eyes. The lack of GV difference may be attributed to enhanced cell matrix connectivity between the inner wall and JCT in human eyes compared with nonhuman eyes; additionally, JCT expansion reduces the resistance at the JCT/inner wall site and may in fact reduce the GV number and/or result in collapse of the GV, as suggested by Ethier et al.,[9] which rendered GV unidentifiable under light microscopy.

Lastly, a potential mechanism that could affect outflow facility is the cellular relaxation in the aqueous outflow pathway induced by Y27632. Rho-kinase is known to phosphorylate MLC by direct phosphorylation of MLC, and also by promoting indirect phosphorylation by decreasing myosin phosphatase activity, resulting in smooth muscle contraction.[36–38] Recent studies have shown that Y27632 caused decreases in cell stiffness in both human TM-[39] and SC-cultured[40] cells, suggesting their roles as modulators of outflow resistance. Our data demonstrated an increased TM thickness (relaxation) in high-tracer regions compared with low-tracer regions and a significant increase in the high-tracer regions following Y27632 treatment, compared to its controls. Therefore, we postulate that the Y27632-induced increase in outflow facility in human eyes could be attributed to the concerted effect of increased TM and JCT expansion, with JCT expansion playing the major role.

In addition, we carefully examined serial sections in multiple SC regions where tracers were found on both basal and apical sides of SC endothelium and found a pore in each of these regions. All pores found in these regions were identified as paracellular pores. These data support the hypothesis that

Investigative Ophthalmology & Visual Science

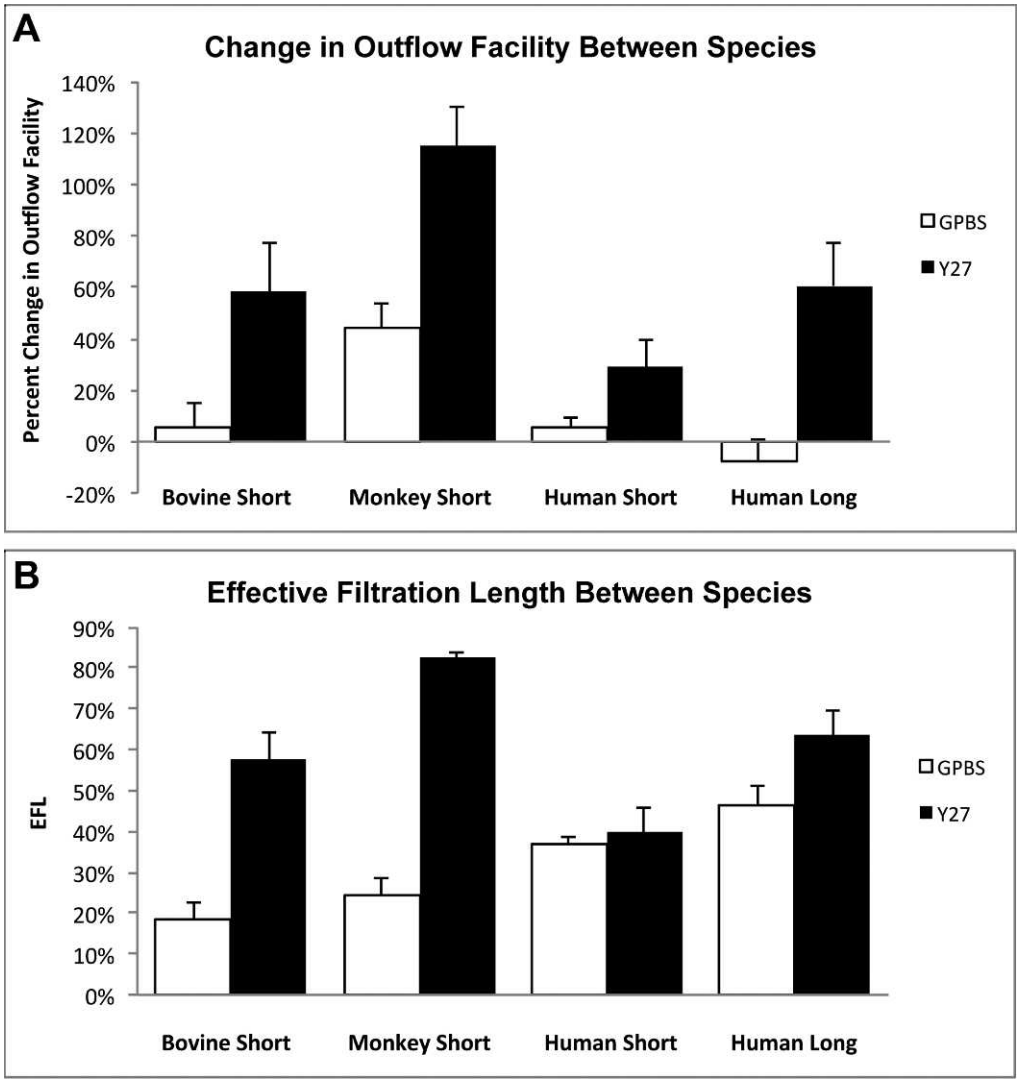

Figure 9. Comparison of outflow facility and effective filtration length in human, bovine, and monkey eyes. (**A**) Percent change in outflow facility in bovine,[14] monkey,[21] and human eyes after Y27632 treatment. Human eyes required a longer perfusion time with Y27632 to achieve the same percent increase in outflow facility as found in bovine eyes when perfused for a short duration, while this increase was still less than the level achieved in monkey eyes when perfused for a short duration with Y27632. (**B**) Percent EFL in bovine,[14] monkey,[21] and human eyes after Y27632 treatment. No change in EFL was found between short-duration Y27632 and its controls. An increase with respect to its controls in EFA after long-duration of Y27632 perfusion in human eyes is smaller compared with short-duration Y27632 treatment in both bovine[14] and monkey[21] eyes.

the paracellular pathway may be the predominant aqueous outflow pathway as indicated by an earlier study using cationized ferritin.[41] A previous study has shown that latrunculin-B treated eyes had increased pore size and density compared with control eyes.[9] However, an in-depth analysis of the size and density of paracellular pores is out of the scope of this study. Future studies will need to determine the effects of Y27632 on paracellular pores and whether pores play a role in contributing to aqueous outflow resistance.

In summary, Y27632 increased outflow facility in human eyes. However, compared with our previous reports in nonhuman eyes, this increase is smaller and took a longer time to reach statistical significance compared with its control groups. Similar to our previous studied in bovine and monkeys, the increase in outflow facility by Y27632 correlates positively with an increase in EFL, which is associated with an increased expansion in the JCT, but to a lesser degree. Our current data in human eyes support our previous results in nonhuman eyes that EFL could serve as a novel parameter to correlate with outflow facility.

Acknowledgments

The authors thank Enhua Zhou for the helpful discussion, and Rozanne Richman for the technical assistance.

Supported by an American Health Assistance Foundation Grant G2009-018, the Boston University School of Medicine Wing Tat Lee Fund, the National Institutes of Health Grants EY018712, EY022634, and The Massachusetts Lions Eye Research Fund.

Disclosure: **C.-Y.C. Yang**, None; **Y. Liu**, None; **Z. Lu**, None; **R. Ren**, None; **H. Gong**, None

References

1. Grant WM. Experimental aqueous perfusion in enucleated human eyes. *Arch Ophthalmol*. 1963;69:783–801.

2. Johnson M. 'What controls aqueous humour outflow resistance?' *Exp Eye Res*. 2006;82:545–557.
3. Tamm ER, Fuchshofer R. What increases outflow resistance in primary open-angle glaucoma? *Surv Ophthalmol*. 2007; 52(suppl 2):S101–S104.
4. Overby DR, Stamer WD, Johnson M. The changing paradigm of outflow resistance generation: towards synergistic models of the JCT and inner wall endothelium. *Exp Eye Res*. 2009;88: 656–670.
5. Gong H, Freddo TF. The washout phenomenon in aqueous outflow–why does it matter? *Exp Eye Res*. 2009;88:729–737.
6. Johnson DH. The effect of cytochalasin D on outflow facility and the trabecular meshwork of the human eye in perfusion organ culture. *Invest Ophthalmol Vis Sci*. 1997;38:2790–2799.
7. Kaufman PL, Erickson KA. Cytochalasin B and D dose-outflow facility response relationships in the cynomolgus monkey. *Invest Ophthalmol Vis Sci*. 1982;23:646–650.
8. Tian B, Gabelt BT, Geiger B, Kaufman PL. Combined effects of H-7 and cytochalasin B on outflow facility in monkeys. *Exp Eye Res*. 1999;68:649–655.
9. Ethier CR, Read AT, Chan DW. Effects of latrunculin-B on outflow facility and trabecular meshwork structure in human eyes. *Invest Ophthalmol Vis Sci*. 2006;47:1991–1998.
10. Sabanay I, Tian B, Gabelt BT, Geiger B, Kaufman PL. Latrunculin B effects on trabecular meshwork and corneal endothelial morphology in monkeys. *Exp Eye Res*. 2006;82: 236–246.
11. Bahler CK, Hann CR, Fautsch MP, Johnson DH. Pharmacologic disruption of Schlemm's canal cells and outflow facility in anterior segments of human eyes. *Invest Ophthalmol Vis Sci*. 2004;45:2246–2254.
12. Sabanay I, Tian B, Gabelt BT, Geiger B, Kaufman PL. Functional and structural reversibility of H-7 effects on the conventional aqueous outflow pathway in monkeys. *Exp Eye Res*. 2004;78: 137–150.
13. Honjo M, Tanihara H, Inatani M, et al. Effects of rho-associated protein kinase inhibitor Y-27632 on intraocular pressure and outflow facility. *Invest Ophthalmol Vis Sci*. 2001;42:137–144.
14. Lu Z, Overby DR, Scott PA, Freddo TF, Gong H. The mechanism of increasing outflow facility by rho-kinase inhibition with Y-27632 in bovine eyes. *Exp Eye Res*. 2008; 86:271–281.
15. Rao PV, Deng PF, Kumar J, Epstein DL. Modulation of aqueous humor outflow facility by the Rho kinase-specific inhibitor Y-27632. *Invest Ophthalmol Vis Sci*. 2001;42:1029–1037.
16. Tian B, Kaufman PL. Effects of the Rho kinase inhibitor Y-27632 and the phosphatase inhibitor calyculin A on outflow facility in monkeys. *Exp Eye Res*. 2005;80:215–225.
17. Waki M, Yoshida Y, Oka T, Azuma M. Reduction of intraocular pressure by topical administration of an inhibitor of the Rho-associated protein kinase. *Curr Eye Res*. 2001;22:470–474.
18. Fukiage C, Mizutani K, Kawamoto Y, Azuma M, Shearer TR. Involvement of phosphorylation of myosin phosphatase by ROCK in trabecular meshwork and ciliary muscle contraction. *Biochem Biophys Res Commun*. 2001;288:296–300.
19. Kaibuchi K, Kuroda S, Amano M. Regulation of the cytoskeleton and cell adhesion by the Rho family GTPases in mammalian cells. *Ann Rev Biochem*. 1999;68:459–486.
20. Rosenthal R, Choritz L, Schlott S, et al. Effects of ML-7 and Y-27632 on carbachol- and endothelin-1-induced contraction of bovine trabecular meshwork. *Exp Eye Res*. 2005;80:837–845.
21. Lu Z, Zhang Y, Freddo TF, Gong H. Similar hydrodynamic and morphological changes in the aqueous humor outflow pathway after washout and Y27632 treatment in monkey eyes. *Exp Eye Res*. 2011;93:397–404.
22. Scott PA, Lu Z, Liu Y, Gong H. Relationships between increased aqueous outflow facility during washout with the changes in hydrodynamic pattern and morphology in bovine aqueous outflow pathways. *Exp Eye Res*. 2009;89:942–949.
23. Erickson-Lamy K, Schroeder AM, Bassett-Chu S, Epstein DL. Absence of time-dependent facility increase ("washout") in the perfused enucleated human eye. *Invest Ophthalmol Vis Sci*. 1990;31:2384–2388.
24. Scott PA, Overby DR, Freddo TF, Gong H. Comparative studies between species that do and do not exhibit the washout effect. *Exp Eye Res*. 2007;84:435–443.
25. Sabanay I, Gabelt BT, Tian B, Kaufman PL, Geiger B. H-7 effects on the structure and fluid conductance of monkey trabecular meshwork. *Arch Ophthalmol*. 2000;118:955–962.
26. Johnson M, Shapiro A, Ethier CR, Kamm RD. Modulation of outflow resistance by the pores of the inner wall endothelium. *Invest Ophthalmol Vis Sci*. 1992;33:1670–1675.
27. Parc CE, Johnson DH, Brilakis HS. Giant vacuoles are found preferentially near collector channels. *Invest Ophthalmol Vis Sci*. 2000;41:2984–2990.
28. Ten Hulzen RD, Johnson DH. Effect of fixation pressure on juxtacanalicular tissue and Schlemm's canal. *Invest Ophthalmol Vis Sci*. 1996;37:114–124.
29. Alvarado JA, Yun AJ, Murphy CG. Juxtacanalicular tissue in primary open angle glaucoma and in nonglaucomatous normals. *Arch Ophthalmol*. 1986;104:1517–1528.
30. Grierson I, Lee WR. Light microscopic quantitation of the endothelial vacuoles in Schlemm's canal. *Am J Ophthalmol*. 1977;84:234–246.
31. Moses RA. Circumferential flow in Schlemm's canal. *Am J Ophthalmol*. 1979;88:585–591.
32. Battista SA, Lu Z, Hofmann S, Freddo T, Overby DR, Gong H. Reduction of the available area for aqueous humor outflow and increase in meshwork herniations into collector channels following acute IOP elevation in bovine eyes. *Invest Ophthalmol Vis Sci*. 2008;49:5346–5352.
33. Swaminathan SS, Oh DJ, Kang MH, et al. Secreted protein acidic and rich in cysteine (SPARC)-null mice exhibit more uniform outflow. *Invest Ophthalmol Vis Sci*. 2013;54:2035–2047.
34. Zhang Y, Toris CB, Liu Y, Ye W, Gong H. Morphological and hydrodynamic correlates in monkey eyes with laser induced glaucoma. *Exp Eye Res*. 2009;89:748–756.
35. Kameda T, Inoue T, Inatani M, et al. The effect of Rho-associated protein kinase inhibitor on monkey Schlemm's canal endothelial cells. *Invest Ophthalmol Vis Sci*. 2012;53: 3092–3103.
36. Amano M, Ito M, Kimura K, et al. Phosphorylation and activation of myosin by Rho-associated kinase (Rho-kinase). *J Biol Chem*. 1996;271:20246–20249.
37. Kimura K, Ito M, Amano M, et al. Regulation of myosin phosphatase by Rho and Rho-associated kinase (Rho-kinase). *Science*. 1996;273:245–248.
38. Kureishi Y, Kobayashi S, Amano M, et al. Rho-associated kinase directly induces smooth muscle contraction through myosin light chain phosphorylation. *J Biol Chem*. 1997;272:12257–12260.
39. Rao PV, Deng P, Sasaki Y, Epstein DL. Regulation of myosin light chain phosphorylation in the trabecular meshwork: role in aqueous humour outflow facility. *Exp Eye Res*. 2005;80: 197–206.
40. Zhou EH, Krishnan R, Stamer WD, et al. Mechanical responsiveness of the endothelial cell of Schlemm's canal: scope, variability and its potential role in controlling aqueous humour outflow. *J R Soc Interface*. 2012;9:1144–1155.
41. Epstein DL, Rohen JW. Morphology of the trabecular meshwork and inner-wall endothelium after cationized ferritin perfusion in the monkey eye. *Invest Ophthalmol Vis Sci*. 1991;32:160–171.

Investigative Ophthalmology & Visual Science